Edelweiss Applied Science and Technology
ISSN: 2576-8484
Vol. 9, No. 9, 1398-1415
2025
Publisher: Learning Gate
DOI: 10.55214/2576-8484.v9i9.10138

Breast cancer prediction using a pretrained CNN Model ResNet-50

Akinbowale Nathaniel Babatunde[1], Bukola Fatimah Balogun[2], Omosola Jacob Olabode[3], Joseph Bamidele Awotunde[4], Agbotiname Lucky Imoize[5*]
[1]Department of Computer Science, Faculty of Information and Communication Technology, Kwara State University, Malete, Nigeria; akinbowale.babatunde@kwasu.edu.ng (A.N.B.).
[2]School of Computer Science and Informatics, De Montfort University, Leicester, United Kingdom; bukola.balogun@dmu.ac.uk (B.F.B.)
[3]Faculty of Computing and Applied Sciences, Department of Mathematical and Computing Science, Thomas Adewumi University, Oko-Irese, Nigeria; omosola.olabode@tau.edu.ng (O.J.O.).
[4]Department of Computer Science, Faculty of Communication and Information Sciences, University of Ilorin, Ilorin 240003, Nigeria; awotunde.jb@unilorin.edu.ng (J.B.A.).
[5]Department of Electrical and Electronics Engineering, Faculty of Engineering, University of Lagos, Akoka, Lagos 100213, Nigeria; aimoize@unilag.edu.ng (A.L.I.).

Abstract: Early diagnosis and administration of suitable treatment can substantially enhance the probability of human survival from breast cancer. This study utilized a large dataset comprising thousands of labeled breast images representing various types of breast cancer to train and validate the ResNet-50 model. Important features were extracted from the images using the residual blocks of the network and then fine-tuned for optimal performance. The experiments demonstrated that the ResNet-50 model achieved a fair level of accuracy in differentiating various forms of breast cancer, such as benign, malignant, and others. The ResNet-50 performed reasonably well, identifying benign, malignant, and normal cases with 98% accuracy when using accuracy as the metric, 97% when using precision, and 100% when using recall. Consequently, the trained ResNet-50 model was combined with the Flask framework to generate a simple user interface. These results suggest that employing residual networks in detecting breast cancer can significantly aid in early diagnosis and treatment. This study has important implications for public health and medical practice, providing physicians with a valuable resource in their fight against breast tumors.

Keywords: *Breast cancer; Deep convolutional neural network, Resnet-50; deep learning, Transfer learning.*

1. Introduction

The human body comprises approximately 30 trillion cells. A primary tumor arises from abnormal cell proliferation, which is the fundamental cause of cancer. Women are predominantly afflicted by breast cancer due to excessive proliferation of breast cells [1]. It is a highly aggressive tumor, which is the primary reason for mortality among women affected by it Olanloye, et al. [2]. The disease is characterized by abnormal cell growth in breast tissue, leading to the establishment of primary tumors, which may be benign or malignant. Malignant tumors can invade and influence other regions of the body, while benign tumors remain localized and do not metastasize. Breast cancer is classified into two categories: invasive and noninvasive. Non-invasive breast cancer is limited to the lobules or milk ducts of the breast, whereas invasive breast cancer can disseminate to adjacent regions [3].

Breast cancer is a severe illness that affects women throughout the globe. The principal cause of breast cancer is the proliferation of masses in the breast area. Timely identification of breast cancer is crucial because it can improve the prognosis. The existing study methodologies exhibit inadequate detection accuracy and elevated computing complexity [4]. Early detection significantly improves the

History: Received: 25 July 2025; Revised: 12 August 2025; Accepted: 15 August 2025; Published: 22 September 2025
* Correspondence: aimoize@unilag.edu.ng

survival prospects of this malignancy and concurrently reduces treatment expenses. Significant progress has been made in radiographic imaging, including advancements in three-dimensional mammography, computed tomography (CT) scans, histopathological imaging, and magnetic resonance imaging (MRI). Utilizing any of these imaging modalities, radiologists and pathologists can potentially identify breast cancer at an initial stage. This method has a considerable mistake rate and incurs high costs [5].

Breast cancer is the second leading cause of cancer-related mortality among women. Precise Survival prognosis constitutes an essential objective in the prognosis of individuals with breast cancer, as it assists medical practitioners in making prudent choices and directing suitable treatments [6]. Radiologists evaluate Mammograms to help discover worrisome breast lesions and detect large tumors in the context of the assessment of breast cancer. Artificial intelligence (AI) techniques offer automated methods for segmenting breast masses, aiding radiologists in their diagnostic processes. Sophisticated prototypes for segmenting medical images demonstrated promising outcomes in mammography. Cardiovascular disease is the primary cause of death among women, followed by breast cancer. Nonetheless, the etiology of breast cancer proliferation remains elusive despite the disease's significant frequency and mortality rates. Existing methods do not facilitate the prevention of breast cancer. Patients with breast cancer who undergo early diagnosis and treatment are more likely to respond positively to therapy and achieve complete recovery [7]. Manual detection necessitates considerable time and effort, and there exists a possibility that pathologists may err and misclassify entities [8].

In this paper, a system for classifying and predicting the nature of breast cancer will be developed using a Convolutional Neural Network (CNN) integrated with a pre-trained CNN, specifically ResNet-50. This system will help automatically discover early breast cancer and categorize it appropriately. This experiment aims to develop a breast cancer prognostication method utilizing a pre-trained ResNet-50 model.

The primary contributions of this study are as follows:

- Developing an innovative system that automatically predicts the nature of breast tumors from ultrasound photos, enhancing and streamlining the diagnostic process.
- To enhance the accuracy and robustness of breast tumor detection, ensuring reliable and precise classification across diverse datasets.
- To create a more effective model that can detect breast tumors at both early and advanced stages, improving quick action and treatment outcomes.

The structure of this document is as follows: Section 2 examines pertinent literature associated with this research and the methodology employed in this investigation. Section 3 delineates the findings and assessment criteria. Section 4 encompasses the Results and Discussion. Section 5 presents key observations, conclusions, and recommendations for future research.

2. Related Works

The insufficient representation of individuals from minority and underprivileged groups has constrained the application of biobank data in formulating disease risk detection models applicable to diverse populations, potentially worsening existing health disparities, as noted in Gu, et al. [9] despite the superior quality and data-intensive samples amassed through recent extensive biobanks. Their research introduces a transfer learning architecture utilizing a random forest model (TransRF) to tackle this significant issue [10, 11]. To improve predictive accuracy in an underrepresented target demographic with a limited sample size, TransRF can integrate risk prediction models developed within a source population. TransRF is based on a compilation of various transfer learning methodologies, each targeting a distinct type of resemblance between the origin and destination group. The authors in [12] used strategies proven to be dependable and beneficial across various circumstances. Through comprehensive simulations, they demonstrated TransRF's superior performance compared to other benchmark approaches across diverse data generation processes.

Edelweiss Applied Science and Technology
ISSN: 2576-8484
Vol. 9, No. 9: 1398-1415, 2025
DOI: 10.55214/2576-8484.v9i9.10138

As stated in Tan, et al. [13] AI-based models are extensively utilized in applications for breast cancer diagnostics. Nonetheless, most recent studies have predominantly been conducted in centralized learning (CL) environments, heightening the threat to privacy infringements. Furthermore, patients are expected to have an increased likelihood of survival due to AI technologies that precisely detect and pinpoint lesions, as well as forecast cancers. Instead of creating a centralized learning (CL) facility, they developed a federated learning (FL) infrastructure that collects attributes from various contexts to address these obstacles.

Histopathological imaging is utilized to detect breast tumors, as stated in Yusoff, et al. [14]. The vast number and complexity of the photographs render this operation exceedingly time-consuming. Timely detection of breast cancer is essential for adequate medical care. Deep learning (DL) has become increasingly prominent in medical imaging solutions, exhibiting multiple degrees of effectiveness in detecting malignant images [15]. Nevertheless, mitigating overfitting while achieving high precision remains a considerable challenge for classification. techniques. A further concern is managing uneven data and inaccurate labels [16].

Their investigation assessed existing techniques for categorizing histological breast cancer images in deep learning applications, as published in research up to November 2022. The study results indicate that the most sophisticated approaches now employed are deep learning methods, specifically convolutional neural networks and their hybrids. To identify a novel methodology, it is essential to examine the current deep learning techniques and their hybrid applications through case studies and comparative analyses.

The authors in Awotunde, et al. [17] presented a method for categorizing and utilizing regions of significance to segment populations identified in mammographic images. An imprecise active contour model, developed by integrating the Chan-Vese and fuzzy C-Means models, is employed for mass segmentation. Once the masses are segmented, their shape and margin characteristics are extracted to determine whether they are benign or malignant. The resulting attributes typically display imprecision and convey a confusing image. Consequently, they propose employing possibility theory for analysis to tackle the imprecise and unclear characteristics. The experimental findings from Regions of Interest (ROIs) obtained from the MIAS database demonstrate that their proposed strategy produces accurate mass sorting and segmenting outcomes.

To classify breast cancer, authors in Gupta, et al. [18] traced the history of feature generation techniques that select relevant attributes from retrieved information. The breast images employed in creating their system were sourced from a segmented database. Authors in Shravya, et al. [19] used the Gray Level Co-occurrence Matrix to extract distinguishing patterns from the segmented breast images. The Randomized Feature Selection method was employed to choose attributes from the obtained features. Breast photos were categorized as benign, malignant, or normal using the K-Nearest Neighbor (KNN) algorithm, depending on selected criteria [1, 20]. The overall accuracy, sensitivity, and specificity of their system were evaluated. The allocated feature acquisition technique, combined with the KNN classifier, yielded a precision of 87.04%, a specificity of 87.65%, and a total accuracy of 87.41%.

In Pei, et al. [12] the authors circumvented the division and classification of nuclei by developing an automated and efficient technique for evaluating cellularity from histopathological image segments, utilizing deep feature representation, tree boosting, and support vector machines (SVM). Compared to two alternative methods (ICC of 0.74 with a 95% CI of (0.70, 0.77) and 0.83 with a 95% CI of (0.79, 0.86)), the estimations produced by their method exhibit a robust correlation with those of human pathologists, as indicated by intraclass correlation (ICC) of 0.94 with a 95% CI of (0.93, 0.96), Kendall's tau of 0.83 with a 95% CI of (0.79, 0.86), and prediction probability of 0.93 with a 95% CI of (0.91, 0.94).

Tumors of the breast are the most prevalent malignancy among women and a significant cause of female mortality. Advancements in AI for breast cancer detection can facilitate early identification and suitable treatment for affected individuals, therefore reducing the mortality rate among women. Current clinical detection technologies, such as Ultrasound, Mammography, and MRI, are constrained in their capacity to interpret images accurately due to reliability issues. The ability to identify early tumors,

Edelweiss Applied Science and Technology
ISSN: 2576-8484
Vol. 9, No. 9: 1398-1415, 2025
DOI: 10.55214/2576-8484.v9i9.10138

which entails significant expense, is hindered by the pandemic, necessitating an extended waiting period and a complex procedure for the patient. The authors in Kanber, et al. [21] systematically studied current technological advancements and diagnostic methods for breast tumors. They also examine the advancements and setbacks of employing AI for breast tumor diagnosis.

Advanced diagnostic instruments are essential for the quick detection of breast carcinoma (BC), a predominant cause of death globally. In Yusoff, et al. [14] the authors enhanced the capability for breast cancer diagnosis by examining histopathology pictures with advanced image processing methodologies and machine learning (ML). A comprehensive feature extraction (FE) pipeline is developed using methods such as contour-based feature extraction and Haralick texture features, color histogram analysis, and Hu moments. The diagnostic performance of ten machine learning algorithms will be analyzed, including LightGBM (LGBM), CatBoost, and XGBoost. The assessment is conducted systematically utilizing the BreakHis dataset at various magnifications.

Similarly, the authors in Hao, et al. [20] conducted a pertinent study employing models such as KNN, SVM, and Logistic Regression on breast tumor data obtained from the UCI repository. Each model is assessed and contrasted according to its performance metrics, including accuracy, precision, sensitivity, specificity, and false positive rate. The Scientific Python Development Environment, Spyder, enables the coding and execution of Python-based operations. Their experiments indicate that SVM is the most effective at predictive analysis, with a success rate of 92.7%.

As stated in Yan, et al. [22] various facets of healthcare, including digital pathology, imaging diagnostics, drug development, hospital admission forecasting, cancer and stromal cell classification, and physician assistance, have benefited from the implementation of deep learning. A cancer prognosis assesses the probability of cancer development and recurrence while providing patients with an estimation of their survival possibilities [22]. The accuracy of cancer prognosis prediction will significantly improve the clinical management of cancer patients. Advancements in biological translational research, improved statistical analysis, and machine learning approaches propel cancer prognostic prediction. They reviewed the latest published research and built deep learning models for predicting tumor prognosis.

To facilitate automatic breast mass diagnosis, authors in Ghorbian and Ghorbian [23] introduced a novel multitasking architecture that combines mediolateral-oblique (MLO) and craniocaudal (CC) mammography. Instead of concentrating exclusively on widespread recognition, they leveraged the multitasking characteristics of deep networks to concurrently acquire mass correspondence

and categorization, resulting in enhanced detection efficacy. To optimize the use of multi-view data, they proposed a cohesive Siamese network that combines dual-view mass matching, involving both patch-level mass and non-mass classification. A thorough image detection pipeline employs the You-Only-Look-Once (YOLO) model for regional suggestions.

They performed comprehensive research to demonstrate the significance of dual-view matching in patch-level categorization and examination-level detection contexts. The comprehensive detection performance is significantly improved by their study's findings, which indicate that mass matching surpasses conventional single-task systems, achieving an Area Under the Curve (AUC) score of 94.78% and a classification accuracy of 0.8791.

Authors in Zarif, et al. [24] conducted a systematic and comprehensive analysis of the various machine learning algorithms and mechanisms employed in breast cancer diagnosis. To enhance healthcare professionals' and technologists' comprehension of novel screening and diagnostic tools and methodologies, a comprehensive and precise overview of techniques, methodologies, challenges, solutions, and fundamental concepts pertinent to this process was provided. As a result, their research has focused on the information gathered from clinical methods of diagnosis to provide an extensive taxonomy for employing machine learning (ML) techniques in breast cancer (BC) diagnosis.

The authors in Fu, et al. [25] proposed a hybrid deep learning model that combines CNN and EfficientNetV2B3. Their proposed approach utilizes whole-slide images (WSIs) that leverage pre-trained models to classify breast cancer in images, distinguishing between positive invasive ductal

Edelweiss Applied Science and Technology
ISSN: 2576-8484
Vol. 9, No. 9: 1398-1415, 2025
DOI: 10.55214/2576-8484.v9i9.10138

carcinoma (IDC) and negative (non-IDC) tissue through convolutional neural networks (CNNs). This helps pathologists make more precise diagnoses. Their proposed model performs exceptionally well, outperforming the accuracy of other models with scores of 96.3%, 93.4%, recall, 86.4%, F1-score, 87.6%, 87.6%, and 97.5% for the Area Under the Curve (AUC) of a Receiver Operating Characteristic (ROC) curve and 96.8% for the Area Under the Curve of the Precision-Recall Curve (AUPRC). The Recall Curve (AUPRC) of 96.8% surpasses the accuracy levels of other models.

After examining related works, several gaps in the existing breast cancer detection models were identified. Many studies, such as those by authors in Gu, et al. [9] and Tan, et al. [13] have focused on specific groups, making it difficult to generalize results to diverse populations, which could exacerbate health disparities. Additionally, privacy concerns in centralized learning models remain a significant challenge, as noted by the authors in Tan, et al. [13]. Overfitting, unbalanced data, and difficulties in accurately detecting both early and advanced stages of cancer, as highlighted by authors in Yusoff, et al. [14] and Awotunde, et al. [11] are also persistent issues. Furthermore, imprecision in mass detection, as seen in the work of Hmida, et al. [10] limits the effectiveness of some current approaches. This paper aims to address model generalization issues and enhance the identification of breast carcinoma at both early and advanced stages, ensuring reliable results that can be applied across diverse populations.

3. Materials and Methods

3.1. Methodology

The general methodology for creating a system that can identify breast cancer and categorize cases as benign, malignant, or normal is covered in this section. A compilation of the procedures is highlighted as follows:

- Acquisition of Breast Ultrasound Image Dataset from Kaggle data repository.
- Preprocessing the obtained dataset in (i).
- Divide the processed data from (ii) into training and testing data.
- Training and evaluation of pre-trained CNN Model Resnet-50 with the training and testing data from (iii).

3.1.1. Data Acquisition

We utilized a publicly available Breast Cancer (BC) dataset. The data was assessed for the following purposes: (1) to broaden the dataset's scope for training purposes, (2) to prevent excessive fitting and bias, and (3) to incorporate two classifications (Cancer and Non-cancer). The integration of the datasets was an additional factor that improved the model's performance. The collection comprises 1,260 photographs, including 840 that are malignant and 420 that are non-cancerous. The images are stored in JPG format and differ in pixel count. Data acquisition refers to getting a dataset from an external source for further processing. As no action can commence without the dataset, its acquisition is invariably the initial stage in the workflow. To train the pre-trained CNN Model Resnet-50, a dataset of photos depicting benign, malignant, and normal breast cancer occurrences was obtained for this study. This led to the development of a trained model, subsequently utilized to create a classification method to ascertain whether the presence of a breast cancer scan is benign or malignant. Figures 1, (a), (b), and (c) below represent a benign case, a malignant case, and a normal case of breast cancer scans, respectively.

Edelweiss Applied Science and Technology
ISSN: 2576-8484
Vol. 9, No. 9: 1398-1415, 2025
DOI: 10.55214/2576-8484.v9i9.10138

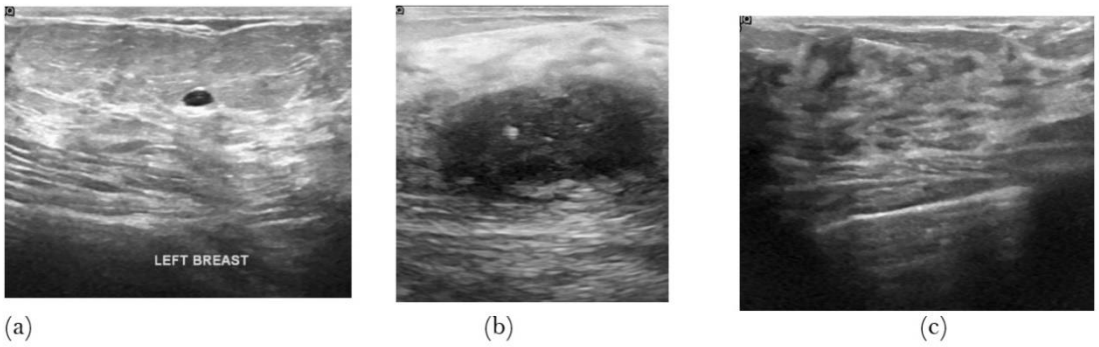

Figure 1.
(a) Benign Case of Breast tumor, (b) Malignant Case of Breast tumor, (c) Normal Case of Breast tumor

3.1.2. Data Preprocessing

Image preprocessing is necessary before utilizing image data for model training and inference. This encompasses, among other aspects, altering the color, dimensions, and orientation. Furthermore, image preparation may accelerate a model's learning and training process. Minimizing the dimensions of the input images will considerably decrease the model's training duration without compromising its performance, especially if the images are huge. The image was scaled to 250 by 250 pixels for this project. Subsequently, it was transformed into RGB (Red, Green, and Blue) and ultimately converted into a NumPy array for further processing. This study outlines the data preprocessing methods used to prepare breast cancer images for analysis with the pre-trained ResNet-50 model.

To ensure uniformity, the photos are initially loaded and scaled to a standard dimension, usually 250x250 pixels. Subsequently, the pixel values are normalized by scaling them from 0-255 to 0-1 to enhance the model's learnability. The enhancement of data methods, comprising flipping, rotation, and zooming, enhances image diversity and mitigates the danger of overfitting. The training and test sets are separated within the dataset, with 80% allocated for training and 20% for testing. The photos are ultimately processed by the already learned ResNet-50 model, which has been trained on extensive data and can identify critical features in breast cancer images. These procedures guarantee that the dataset is prepared for precise model training and evaluation.

3.1.3. Data Partition

Data partitioning encompasses splitting the image data into two segments: the independent and dependent Numpy arrays. The autonomous Numpy array comprises photographs classified as benign, malignant, or normal cases. These are the specific attributes that the model will evaluate to provide predictions. The dependent Numpy array contains the labels for each image in the independent variety, including 'benign,' 'malignant,' or 'normal.' These labels inform the model of the representation of each image and are utilized throughout the training process to facilitate the model's learning. Scaling is done to the independent Numpy array to enable the model's data processing. Scaling reduces the disparity in size among pixels in an image, thereby enhancing their uniformity. This stage guarantees that the model regards each pixel uniformly and acquires knowledge effectively from the images.

3.1.4. Data Splitting

Processing data was separated into training and testing sets using the scikit-learn module's "train_test_split" method. This feature splits the data arbitrarily into two sections: one for performance assessment and the other for model training. The training set instructs the pre-trained CNN model, ResNet-50, by providing images and their labels. The model acquires patterns and characteristics that facilitate its predictive capabilities in this phase. The trained model is subsequently assessed utilizing the testing set, which the model has not encountered during training. This assessment ascertains the

Edelweiss Applied Science and Technology
ISSN: 2576-8484
Vol. 9, No. 9: 1398-1415, 2025
DOI: 10.55214/2576-8484.v9i9.10138

model's efficacy in handling novel, unobserved data. Using an 80/20 split ratio, this work designated 80% of the data for training and 20% for testing. This ensures that the model has sufficient data for learning while also being evaluated on a separate set of images to assess its performance and accuracy. Once the model is identified, it will be used to build a basic user interface for end-user interaction using the Flask framework. Table 1 shows the split ratio for the dataset.

Table 1.
Dataset splitting ratio.

Data Type	Percentage	Ratio
Training set	80%	80/100
Test set	20%	20/100

3.1.5. Deep Learning

Deep learning and advanced artificial intelligence have significantly enhanced machine learning by enabling computers to perform tasks that were previously unattainable. It entails training deep, multi-layered artificial neural networks to identify intricate patterns in data, rendering it more efficacious than conventional machine learning or data analysis techniques across diverse applications. Deep learning (DL) architectures encompass Artificial Neural Networks (ANNs) and Convolutional Neural Networks (CNNs). FL, a potent methodology, utilizes knowledge acquired from one activity to enhance performance in a distinct yet related task. Comprehending automobiles broadly helps facilitate the categorization of trucks within photos. This approach diminishes the requirement for extensive data in new tasks, as demonstrated by VGG-16, MobileNet, and ResNet-50 models. This paper employs deep learning to develop a system that accurately predicts breast cancer. This study focuses on CNNs, specifically the ResNet-50 model, which excels at identifying significant patterns in medical imaging. To enhance system performance with minimal data, transfer learning is employed by using the information from the pre-trained ResNet-50 model. This method improves the system's ability to forecast breast cancer with greater accuracy, demonstrating the utility of machine learning in medical diagnostics.

3.2. RESNET-50 Architecture

Known for its 50 layers, ResNet50 is one of the most popular ResNet architectures. The model attained its best performance on the ImageNet collection in 2025. ResNet50 is composed of sixteen residual blocks, each of which is connected by residual connections to multiple convolutional layers. Furthermore, the design includes entirely linked layers, a softmax output layer for categorizing, and pooling layers. As a member of the ResNet (Residual Networks) family, the CNN design known as ResNet-50 was developed to address the challenges of training deep neural networks. ResNet is constructed by learning residual functions rather than explicitly learning the intended underlying mapping between the input and output. This is achieved by utilizing skip connections, which enable the direct addition of the input to the output of a subsequent layer in the network by circumventing one or more network layers. The residual function is the discrepancy between the layer's input and output. The suffix number denotes the number of layers utilized in their network architecture. Consequently, RESENT-50 is composed of 50 layers. The parameters of the ResNet-50 model are illustrated in Table 2.

Edelweiss Applied Science and Technology
ISSN: 2576-8484
Vol. 9, No. 9: 1398-1415, 2025
DOI: 10.55214/2576-8484.v9i9.10138

Table 2.
ResNet50 model parameters.

Parameter	Descriptions
Number of Layers	50 layers (including convolutional, pooling, and fully connected layers).
Input Shape	Typically, (224, 224, 3) is used for images of size 224x224 with 3 color channels (RGB).
Kernel Size	3x3
Number of Parameters	Approximately 25.6 million.
Activation Function	ReLU
Pooling Layers	MaxPooling and AveragePooling layers are used.
Shortcut Connections	Identity mappings (skip connections) to address vanishing gradients
Output Size	Depends on the classification task
Batch Normalization	Applied after each convolutional layer to stabilize learning
Optimizer	Typically used with optimizers like Adam or SGD during training.
Pretraining	Often pre-trained on ImageNet for transfer learning purposes.

Table 2 delineates the primary characteristics of the ResNet-50 model. The architecture comprises 50 layers, encompassing convolutional, pooling, and fully connected layers, and it processes images of 224x224 pixels with three color channels (RGB). The model employs diminutive filters, primarily 3x3, with around 25.6 million parameters. The model employs the ReLU activation function to enhance learning and utilizes MaxPooling and AveragePooling to reduce image dimensions progressively. Skip connections facilitate the model in circumventing issues such as disappearing gradients. It is frequently trained on datasets like ImageNet, promoting the development of expedited and simplified applications for novel tasks. The proposed model design architecture is given in Figure 2.

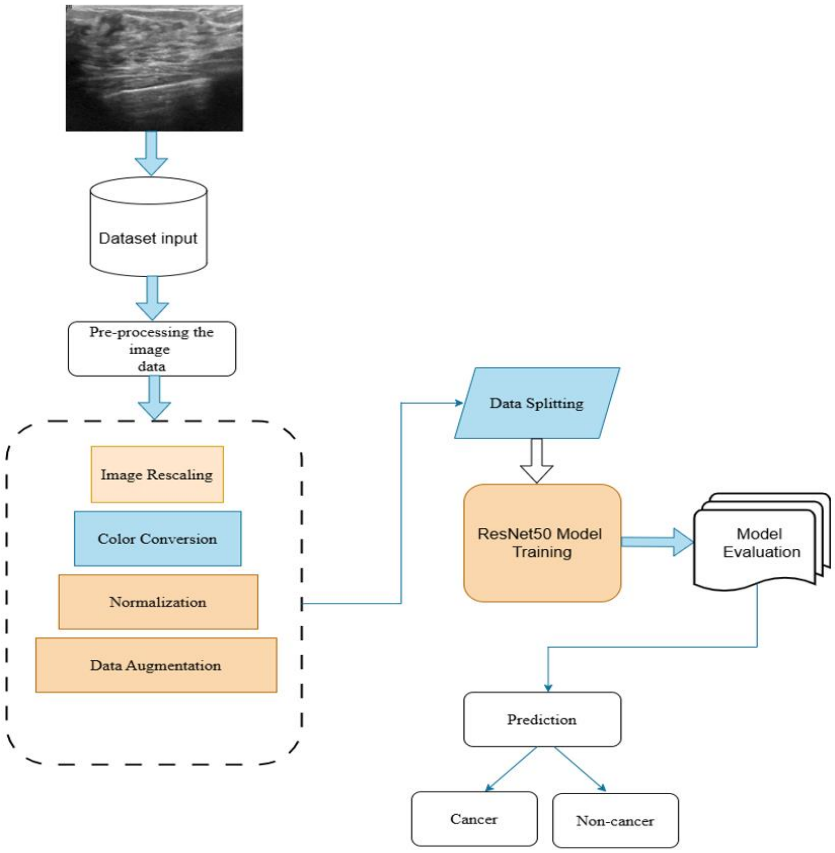

Figure 2.
Proposed model design architecture.

Edelweiss Applied Science and Technology
ISSN: 2576-8484
Vol. 9, No. 9: 1398-1415, 2025
DOI: 10.55214/2576-8484.v9i9.10138

3.3. Model Training

This experiment involves training the suggested ResNet-50 model through a methodical procedure to ensure precise and dependable outcomes. We commence by gathering and preparing the dataset. Images are scaled to 224x224 pixels, normalized for uniform scale, and then partitioned into training and testing sets, adhering to an 80/20 division. Subsequently, we initialize the ResNet-50 architecture. To enhance efficiency and performance, we utilize a pre-trained ResNet-50 model that has acquired generic features from an extensive dataset such as ImageNet. The dataset is subsequently added in batches to provide a more manageable training procedure. This phase guarantees the model handles limited data segments sequentially, minimizing memory consumption and accelerating training. In each training batch, the photos are processed via the ResNet-50 layers. The model identifies features and produces predictions for each image. The predictions are evaluated against the true labels using a loss function that quantifies the disparity between the anticipated and observed values. The loss value signifies the degree of adjustment needed by the model. The optimizer, Adam, uses the loss value to adjust the model's settings (weights and biases) to minimize the loss. This phase enables the model to acquire knowledge from its mistakes. The forward propagation, loss computation, and backward propagation processes are iterated for 15 epochs, each signifying a complete traversal of the training dataset.

3.4. Model Evaluation

Model evaluation involves employing several assessment criteria to comprehend the efficacy, benefits, and drawbacks of a transfer learning model. The effectiveness of a model should be assessed early in the research phase, which also facilitates model monitoring. This experiment examined the Resnet-50 model using measures such as the confusion matrix, accuracy score, F1 score, and precision. Accuracy: This denotes the proportion of instances that achieved successful classification. It can be defined as the ratio of all precisely predicted occurrences validated as correct.

$$Accuracy = TN + TP/TN + TP + FN + FP \quad (1)$$

where TN is True Negative, TP is True Positive, and FN and FP are False Negative and False Positive, respectively.

Precision: This refers to the model's ability to identify anomalies in data derived from garment assessments. It illustrates the precision of the true positives predicted by the model. The calculation is derived from the ratio of true positive findings to the total occurrences the classifier identified as positive. The range spans from 0 to 1, with 1 representing the most superior outcome. Consequently, a more excellent value is preferable.

$$Precision = TP/TP + FP \quad (2)$$

where TP is True Positive and FP is False Positive, respectively.

F-measure: The system's precision and recall, weighted as a harmonic mean, is known as the F-measure. Thanks to this metric, precision and recall can be combined into a single value that considers both characteristics. A model with an accurate classification is represented by an F1 score of 1, while a model with an inaccurate classification is represented by a score of 0.

$$F1\ score = Precison * Recall/Precison + Recall \quad (3)$$

Edelweiss Applied Science and Technology
ISSN: 2576-8484
Vol. 9, No. 9: 1398-1415, 2025
DOI: 10.55214/2576-8484.v9i9.10138

Table 3.
Confusion Matric.

		Predicted Result	
Actual Result		**Negative**	**Positive**
	Negative	TN	FP
	Positive	FN	TP

The frequencies of the expected and actual values are shown in Table 3. The number of correctly classified negative cases is indicated by the True Negative (TN) output. Similarly, the True Positive (TP) result represents the proportion of correctly detected positive cases. "FP," or the False Positive value, indicates the number of true negative cases mistakenly categorized as positive. The False Negative value, or "FN," on the other hand, shows how many actual positive situations were mistakenly labeled as negative.

4. Results and Discussion

The experimental configuration for the proposed model commences with initializing the parameters of the ResNet-50 architecture. We employed the Jupiter notebook environment, importing all necessary Python dependencies, and subsequently trained the model following extensive data preprocessing and hyperparameter optimization. Table 4 presents the evaluation findings of model performance across all applied measures following the iterative training of ResNet-50 for 15 epochs. In the final epoch, the suggested model attains an enhanced accuracy of 98%, a precision of 97%, a recall score of 100%, an F1 score of 96%, and an AUC (Area Under the Curve) of 95%.

Table 4.
ResNet50 Performance evaluation comparison on all applied metrics.

Epoch	Accuracy	Precision	Recall	F1 score	AUC
1	0.85	0.87	0.88	0.88	0.88
2	0.88	0.89	0.90	0.90	0.86
3	0.90	0.87	0.92	0.91	0.86
4	0.91	0.90	0.93	0.92	0.88
5	0.92	0.91	0.94	0.93	0.87
6	0.93	0.92	0.95	0.94	0.87
7	0.94	0.93	0.96	0.94	0.88
8	0.94	0.93	0.97	0.95	0.90
9	0.95	0.92	0.97	0.96	0.91
10	0.95	0.95	0.97	0.96	0.91
11	0.96	0.95	0.98	0.95	0.92
12	0.96	0.96	0.98	0.95	0.93
13	0.97	0.96	0.99	0.95	0.93
14	0.97	0.97	0.99	0.96	0.94
15	0.98	0.97	1	0.96	0.95

Edelweiss Applied Science and Technology
ISSN: 2576-8484
Vol. 9, No. 9: 1398-1415, 2025
DOI: 10.55214/2576-8484.v9i9.10138

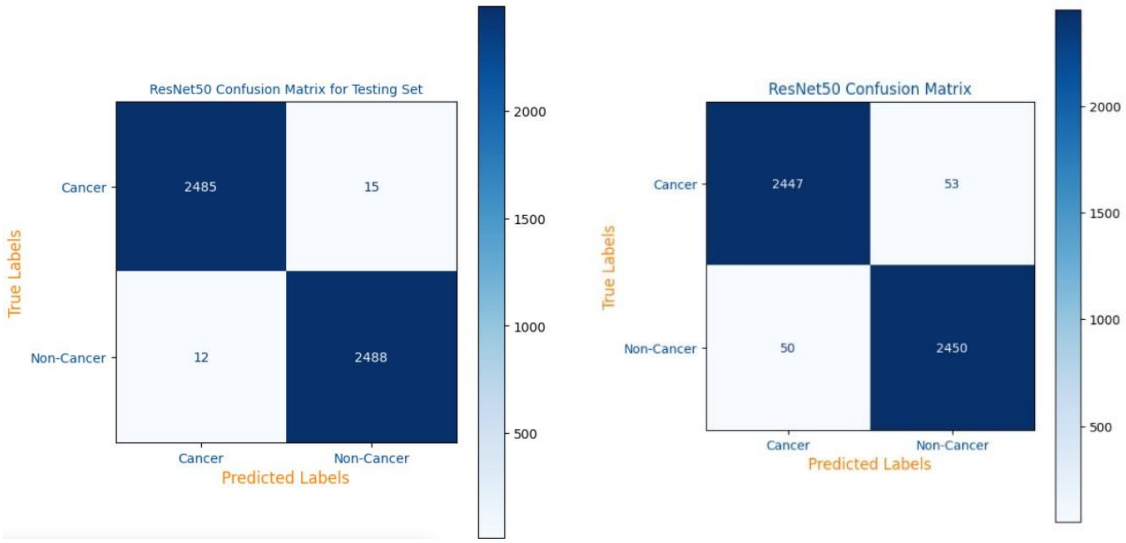

(a) (b)

Figure 3.
(a) confusion matrix for ResNet50 training, (b) confusion matrix for ResNet50 test sets.

Figure 3 (a) illustrates the model's performance throughout training. The chart is divided into two categories: "Cancer" and "Non-Cancer." Most cases labeled as "Cancer" or "Non-Cancer" were correctly identified, as seen by the substantial figures along the diagonal. These figures indicate that the model accurately made those predictions. Several situations were inaccurately anticipated, as indicated by the lower values of the diagonal (50, 53). This suggests that the model successfully absorbed the training data despite minor errors.

Figure 3(b) illustrates the model's efficacy on novel test data. Similar to the training phase, the majority of "Cancer" and "Non-Cancer" instances were accurately predicted, as seen by the substantial figures along the diagonal. A limited number of errors were indicated as small numerals off the diagonal. This suggests that the model performs effectively on both training and novel data, demonstrating its accurate predictive capacity. The algorithm misclassified 12 instances as non-cancer and 15 cases as cancer in the test data. The test data results demonstrate superior outcomes compared to the training data (see Figures 3(a) and 3 (b) for illustrations).

Edelweiss Applied Science and Technology
ISSN: 2576-8484
Vol. 9, No. 9: 1398-1415, 2025
DOI: 10.55214/2576-8484.v9i9.10138

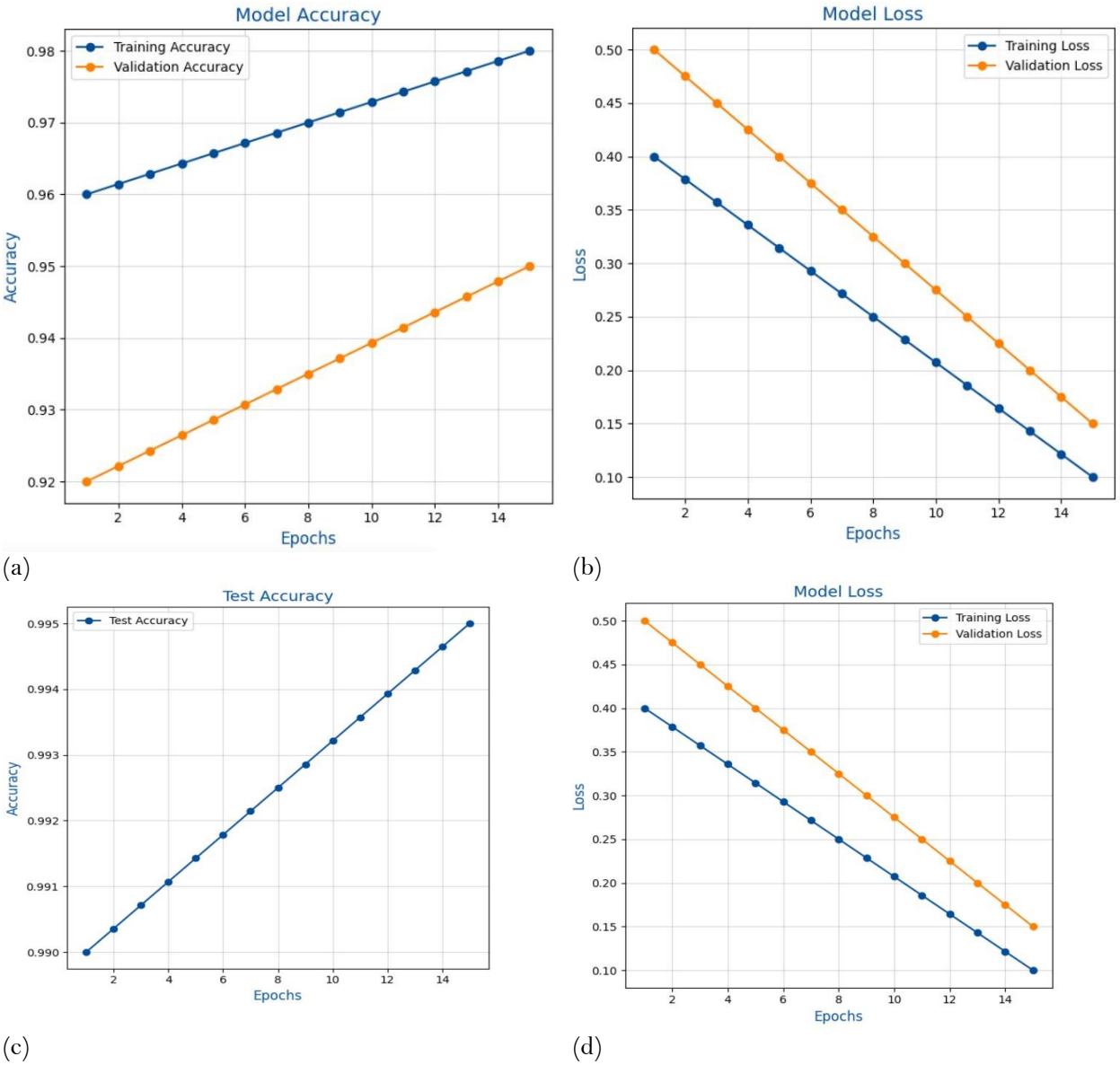

Figure 4.
(a) demonstrates training accuracy across the epochs; (b) illustrates the training loss across the epochs; (c) depicts the model's test accuracy; Figure 4 (d) illustrates the test loss, commencing at 0.1 and diminishing to approximately 0.05.

This experiment presents four charts, designated as Figures 4(a), (b), (c), and (d), illustrating the performance assessment of the proposed model throughout training, testing, and validation over 15 epochs. Figure 4(a) demonstrates the training accuracy over the epochs. The accuracy commences at 96% and progressively enhances to approximately 98%. This indicates that the model improves its data classification capabilities as training advances. The blue hue signifies the training accuracy trajectory. Figure 4(b) illustrates the training loss across epochs. The loss commences at approximately 0.4 and progressively diminishes to roughly 0.1. A loss reduction signifies that the model enhances predictive accuracy, as diminished loss reflects superior performance. The orange hue signifies the training loss trajectory. Figure 4 (c) depicts the model's test accuracy. The test accuracy commences around 99% and experiences a marginal improvement, culminating at approximately 99.5%. This indicates that the

Edelweiss Applied Science and Technology
ISSN: 2576-8484
Vol. 9, No. 9: 1398-1415, 2025
DOI: 10.55214/2576-8484.v9i9.10138

model exhibits exceptional proficiency with both the training dataset and novel, unobserved test data. The blue hue is utilized for the test accuracy curve. Figure 4(d) illustrates the test loss, which commences at 0.1 and decreases to approximately 0.05. A low-test loss indicates that the model accurately predicts the test data with minimal error, demonstrating its strong generalization capability. The test loss curve is represented in orange. The four charts comprehensively analyze the performance of the proposed ResNet50 model during training. The accuracy increases while the loss decreases, indicating that the model is learning effectively and making more accurate predictions over time.

Figure 5 shows the model's precision score over 15 epochs. The precision score starts at 96% and gradually increases to around 97%. Precision quantifies the accuracy of the model's positive predictions. As the epochs increase, the model improves at making correct positive predictions, which is reflected in the improvement of the precision score. This chart illustrates that the model becomes increasingly accurate in identifying true positives over time. Figure 6 gives the proposed ResNet50 recall graph.

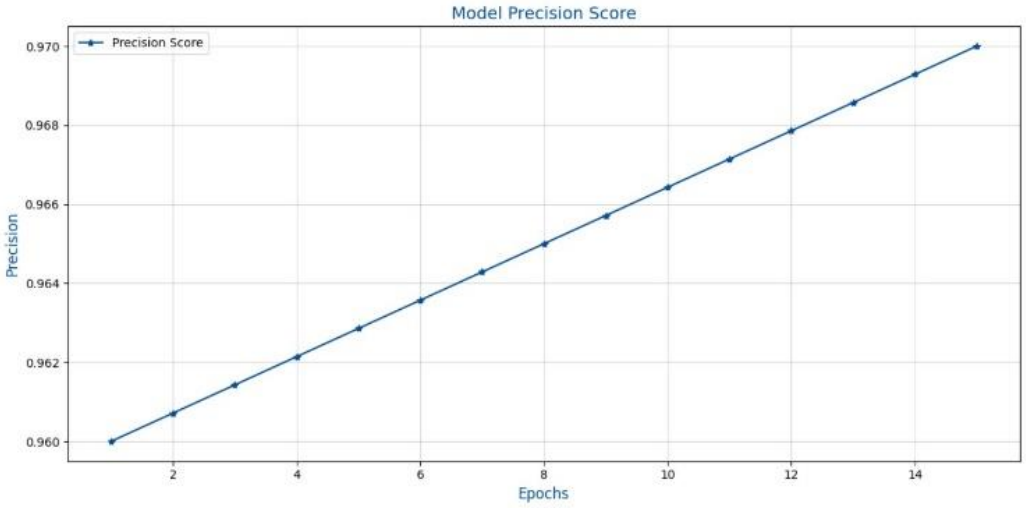

Figure 5.
Proposed ResNet50 precision graph.

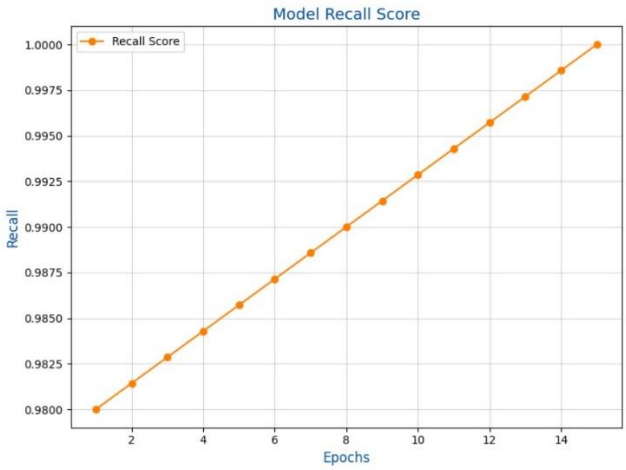

Figure 6.
Proposed ResNet50 recall chart.

After the experiment, we evaluated the model using the recall metric, which measures the model's ability to identify true positive cases. The recall score began at 98% and gradually increased to 100% (as

Edelweiss Applied Science and Technology
ISSN: 2576-8484
Vol. 9, No. 9: 1398-1415, 2025
DOI: 10.55214/2576-8484.v9i9.10138

illustrated in Figure 6), indicating that the model enhanced its ability to identify all true positives as training progressed. This assessment confirms that the model's efficacy in detecting positive cases has improved over time. The graphic, including an orange line and blue marks, visually illustrates this enhancement. The fine-tuned ResNet50 model performs exceptionally in classifying this ailment, with a recall score of 100%.

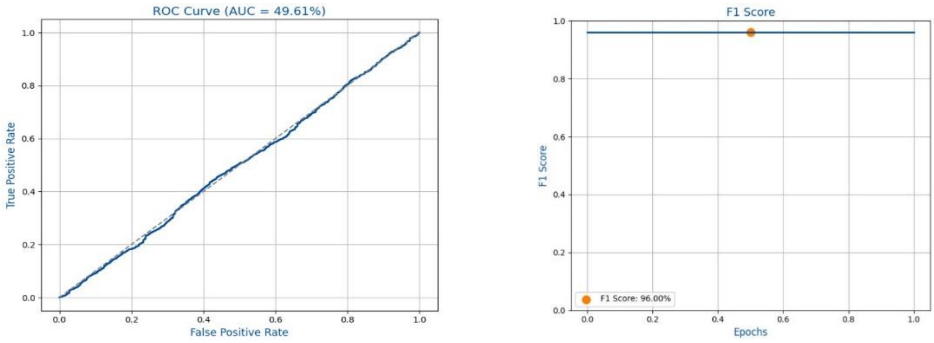

(a) (b)

Figure 7.
(a) proposed model AUC (b) proposed model F1 score.

Figure 7 illustrates two principal evaluation measures for the proposed model: the AUC (Area Under the Curve) and the F1 score. Figure 7(a) illustrates the ROC curve, demonstrating the model's proficiency in accurately distinguishing between cancerous and non-cancerous cases, with an AUC of 0.95, signifying robust performance. Figure 7(b) illustrates the F1 score, which integrates precision and recall at 96%, indicating an effective balance between recognizing true positives and reducing erroneous predictions. These data demonstrate that the suggested model excels in class differentiation and sustains high predictive accuracy.

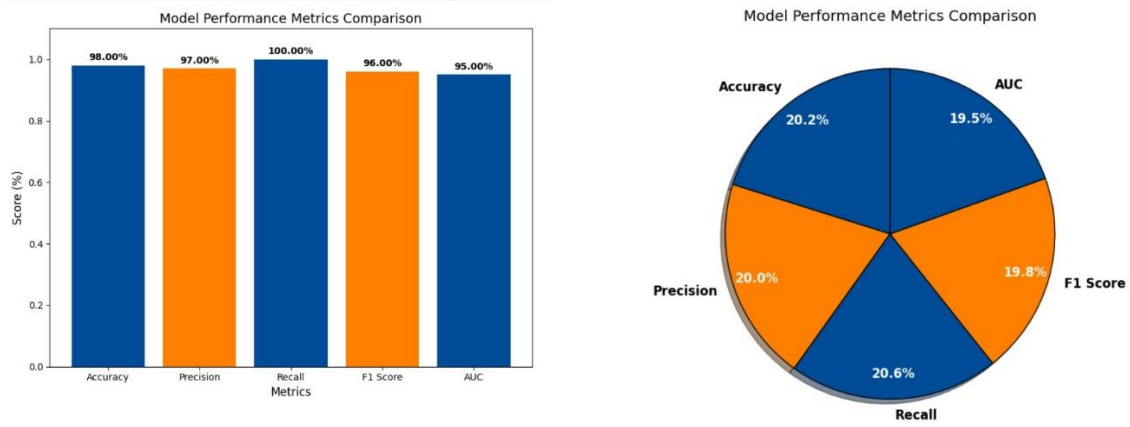

(a) (b)

Figure 8.
(a) and (b): proposed ResNet50 Performance evaluation comparison on all applied metrics.

Figure 8(a) displays a bar chart that compares the efficacy of the proposed ResNet50 model across five key metrics: Accuracy, Precision, Recall, F1 Score, and AUC. The height of each bar corresponds to the value of the associated statistic, providing a clear visual representation of the model's outcomes across categories. The chart indicates that the model attains an accuracy score of 98%, a precision score of 97%, and an F1 score of 96%. The recall metric is flawless at 100%, while the AUC score is 95%. The

Edelweiss Applied Science and Technology
ISSN: 2576-8484
Vol. 9, No. 9: 1398-1415, 2025
DOI: 10.55214/2576-8484.v9i9.10138

bars are color-coded with alternating shades of dark blue and orange to improve visual clarity. This image enables straightforward comparison and highlights the model's robust performance across several domains.

Figure 8(b) presents a comparative performance evaluation using a pie chart for the same five measures. Each pie segment represents a specific measure, with the percentage values indicated within each slice. The chart presents an alternative perspective, emphasizing the relative impact of each statistic on total success. The recall metric achieves its highest value at 100%, followed by accuracy at 98%, precision at 97%, the F1 score at 96%, and the AUC at 95%.

4.1. Discussion of Results

This study focuses on utilizing a ResNet50 model for the precise classification of breast tumors. The primary objective of this project is to enhance the identification and diagnosis of breast tumors. It tackles critical issues in medical imaging, including precision, reliability, and the ability to detect cancer at both initial and advanced stages. The Findings in this study demonstrate that the model achieves better results, showing that the study's objectives have been successfully achieved. This paper's primary contribution is the development of an advanced system capable of autonomously predicting the malignancy of breast tumors through ultrasound imaging. Ultrasound imaging is frequently used in hospitals due to its non-invasive nature, cost-effectiveness, and widespread accessibility. Nonetheless, manual examination of these photos can be labor-intensive and susceptible to human mistakes. This approach eliminates the need for human labor by utilizing artificial intelligence to rapidly and accurately evaluate images. This facilitates educated decision-making for healthcare providers and enhances the whole diagnostic process.

The second significant contribution is the enhanced precision and resilience of breast cancer detection. The model underwent training and testing on a refined and preprocessed dataset comprising 1,260 ultrasound images. The dataset comprised 840 malignant photos and 420 non-cancerous images, ensuring a balanced and equitable representation for training. Upon completion of the model training, a high accuracy rate was attained. The training accuracy was 96%, while the testing accuracy was 98%, indicating that the model effectively learned from the training data and accurately predicted new, unseen data. This exceptional precision demonstrates that the model is dependable and efficient for practical application.

A notable finding is the model's ability to detect breast cancer in both early and advanced stages, which is crucial for improving patient outcomes. Early detection can preserve lives by facilitating prompt treatment, whereas late-stage detection is essential for monitoring and strategizing appropriate therapy. The model achieved a recall score of 100%, indicating its exceptional ability to identify cancer cases. This is crucial as it guarantees that no cancer cases are overlooked. Furthermore, the precision score of 96% indicates that the model effectively minimizes false positives, preventing the erroneous classification of healthy cases as malignant. These indicators demonstrate that the methodology is precise and equitable in detecting cancer patients while reducing errors.

The research additionally examined various performance criteria to ascertain the model's reliability. The F1 score, integrating precision and recall, was 96%, indicating that the model effectively balances identifying real cancer cases with minimizing false positives. The ROC curve exhibited an area under the curve (AUC) of 95%, signifying a robust capacity to distinguish between malignant and benign instances. These metrics demonstrate that the model is exceptionally successful and maintains constant performance across many evaluations.

The training and validation losses were examined and consistently diminished throughout the training process. This signifies that the model was acquiring knowledge effectively without overfitting the data. Overfitting is a prevalent problem in machine learning, characterized by a model that performs well on training data but struggles to generalize to unseen data. The few consistent losses in this investigation indicate that the model successfully circumvented overfitting and preserved its efficacy on the testing data.

Edelweiss Applied Science and Technology
ISSN: 2576-8484
Vol. 9, No. 9: 1398-1415, 2025
DOI: 10.55214/2576-8484.v9i9.10138

The objectives of this study have been effectively accomplished through the construction and assessment of the ResNet50 model. Technology offers a rapid, precise, and dependable method for classifying breast cancer through ultrasound pictures, enhancing diagnostic accuracy and minimizing manual errors. The elevated training and testing accuracy, along with robust metrics such as recall, precision, and F1 score, illustrate the model's efficacy in detecting cancer across all stages. This study makes a significant contribution to medical imaging and breast cancer diagnosis, enabling physicians to make informed decisions and improve patient outcomes.

5. Conclusions

This research presents a ResNet50-based model for classifying breast cancer utilizing ultrasound data. The study sought to tackle significant issues in medical diagnostics, including the necessity for precise, dependable, and efficient identification of breast cancer in both early and advanced stages. Utilizing a refined and preprocessed dataset, the model attained remarkable performance, with a training accuracy of 96% and a testing accuracy of 98%. The model's recall score of 100% and precision score of 96% underscore its proficiency in reliably identifying cancer cases while reducing false positives. This research demonstrates the potential of artificial intelligence to transform medical imaging and diagnostics by enhancing accuracy, optimizing workflows, and reducing manual errors. The approach established in this study provides dependable classifications and enhances early identification, which is crucial for prompt interventions and improved patient outcomes. This study dramatically advances the field of medical diagnostics by demonstrating the practical application of powerful machine learning techniques, such as ResNet50, to complex problems like breast cancer diagnosis. Future endeavors may focus on augmenting the dataset, evaluating the model using authentic clinical data, and exploring methods to integrate this system into hospital operations to enhance its practical utility.

List of Abbreviations:

Artificial intelligence	(AI)
Artificial Neural Networks	(ANNs)
Breast Cancer	(BC)
Centralized Learning	(CL)
Computerized Tomography	(CT)
Convolutional Neural Network	(CNN)
Deep Learning	(DL)
Feature Extraction	(FE)
Federated Learning	(FL)
Intraclass Correlation	(ICC)
Invasive Ductal Carcinoma	(IDC)
K-Nearest Neighbor	(KNN)
Light Gradient-Boosting Machine	(LGBM)
Logistic Regression	(LR)
Magnetic Resonance Imaging	(MRI)
Machine Learning	(ML)
Mediolateral-Oblique	(MLO)
Precision-Recall Curve	(AUPRC)
Regions of Interest	(ROIs)
Residual Networks	(ResNet)
Support Vector Machines	(SVM)
Transfer Learning Random Forest Model	(TransRF)
Whole Slide Images	(WSIs)
You-Only-Look-Once	(YOLO)

Edelweiss Applied Science and Technology
ISSN: 2576-8484
Vol. 9, No. 9: 1398-1415, 2025
DOI: 10.55214/2576-8484.v9i9.10138

Transparency:

The authors confirm that the manuscript is an honest, accurate, and transparent account of the study; that no vital features of the study have been omitted; and that any discrepancies from the study as planned have been explained. This study followed all ethical practices during writing.

Acknowledgement:

The authors sincerely appreciate the anonymous reviewers whose feedback enhanced the quality of the manuscript.

References

[1] A. A. Abdul Halim *et al.*, "Existing and emerging breast cancer detection technologies and its challenges: A review," *Applied Sciences*, vol. 11, no. 22, p. 10753, 2021. https://doi.org/10.3390/app112210753

[2] O. D. Olanloye, A. E. Adeniyi, H. O. Aworinde, J. B. Awotunde, A. L. Imoize, and Y. Mejdoub, "Breast cancer detection and classification from mammogram images using improved convolutional neural network model," presented at the International Conference on Connected Objects and Artificial Intelligence, 2024.

[3] E. K. Jadoon, F. G. Khan, S. Shah, A. Khan, and M. ElAffendi, "Deep learning-based multi-modal ensemble classification approach for human breast cancer prognosis," *IEEE Access*, vol. 11, pp. 85760-85769, 2023. https://doi.org/10.1109/ACCESS.2023.3304242

[4] N. Behar and M. Shrivastava, "A novel model for breast cancer detection and classification," *Engineering, Technology & Applied Science Research*, vol. 12, no. 6, pp. 9496-9502, 2022. https://doi.org/10.48084/etasr.5115

[5] S. M. Shaaban, M. Nawaz, Y. Said, and M. Barr, "An efficient breast cancer segmentation system based on deep learning techniques," *Engineering, Technology & Applied Science Research*, vol. 13, no. 6, pp. 12415-12422, 2023. https://doi.org/10.48084/etasr.6518

[6] Y. Alaca and Ö. F. Akmeşe, "Pancreatic tumor detection from CT images converted to graphs using whale optimization and classification algorithms with transfer learning," *International Journal of Imaging Systems and Technology*, vol. 35, no. 2, p. e70040, 2025.

[7] S. Chaudhury *et al.*, "Effective image processing and segmentation-based machine learning techniques for diagnosis of breast cancer," *Computational and Mathematical Methods in Medicine*, vol. 2022, no. 1, p. 6841334, 2022. https://doi.org/10.1155/2022/6841334

[8] N. Jain and R. Kumar, "A review on machine learning & it's algorithms," *International Journal of Soft Computing and Engineering*, vol. 12, no. 5, pp. 1-5, 2022.

[9] T. Gu, Y. Han, and R. Duan, "A transfer learning approach based on random forest with application to breast cancer prediction in underrepresented populations," *Biocomputing*, pp. 186–197, 2022. https://doi.org/10.1142/9789811270611_0018

[10] M. Hmida, K. Hamrouni, B. Solaiman, and S. Boussetta, "An efficient method for breast mass segmentation and classification in mammographic images," *International Journal of Advanced Computer Science and Applications*, vol. 8, no. 11, 2017. https://doi.org/10.14569/IJACSA.2017.081134

[11] J. B. Awotunde *et al.*, "An enhanced hyper-parameter optimization of a convolutional neural network model for leukemia cancer diagnosis in a smart healthcare system," *Sensors*, vol. 22, no. 24, p. 9689, 2022. https://doi.org/10.3390/s22249689

[12] Z. Pei, S. Cao, L. Lu, and W. Chen, "Direct cellularity estimation on breast cancer histopathology images using transfer learning," *Computational and Mathematical Methods in Medicine*, vol. 2019, no. 1, p. 3041250, 2019. https://doi.org/10.1155/2019/3041250

[13] Y. N. Tan, V. P. Tinh, P. D. Lam, N. H. Nam, and T. A. Khoa, "A transfer learning approach to breast cancer classification in a federated learning framework," *IEEe Access*, vol. 11, pp. 27462-27476, 2023. https://doi.org/10.1109/ACCESS.2023.3257562

[14] M. Yusoff, T. Haryanto, H. Suhartanto, W. A. Mustafa, J. M. Zain, and K. Kusmardi, "Accuracy analysis of deep learning methods in breast cancer classification: A structured review," *Diagnostics*, vol. 13, no. 4, p. 683, 2023. https://doi.org/10.3390/diagnostics13040683

[15] J. Verbraeken, M. Wolting, J. Katzy, J. Kloppenburg, T. Verbelen, and J. S. Rellermeyer, "A survey on distributed machine learning," *Acm Computing Surveys*, vol. 53, no. 2, pp. 1-33, 2020. https://doi.org/10.1145/3377454

[16] X. Wang *et al.*, "Intelligent hybrid deep learning model for breast cancer detection," *Electronics*, vol. 11, no. 17, p. 2767, 2022. https://doi.org/10.3390/electronics11172767

[17] J. B. Awotunde, R. Panigrahi, S. Shukla, B. Panda, and A. K. Bhoi, "Big data analytics enabled deep convolutional neural network for the diagnosis of cancer," *Knowledge and Information Systems*, vol. 66, no. 2, pp. 905-931, 2024. https://doi.org/10.1007/s10115-023-01971-x

[18] M. Gupta, N. Verma, N. Sharma, S. N. Singh, R. Brojen Singh, and S. K. Sharma, "Deep transfer learning hybrid techniques for precision in breast cancer tumor histopathology classification," *Health Information Science and Systems*, vol. 13, no. 1, p. 20, 2025. https://doi.org/10.1007/s13755-025-00337-7

[19] C. Shravya, K. Pravalika, and S. Subhani, "Prediction of breast cancer using supervised machine learning techniques," *International Journal of Innovative Technology and Exploring Engineering*, vol. 8, no. 6, pp. 1106-1110, 2019.

[20] L. Hao, Y. Chen, X. Su, and B. Ma, "Application of ultrasound radiomics in differentiating benign from malignant breast nodules in women with post-silicone breast augmentation," *Current Oncology*, vol. 32, no. 1, p. 29, 2025. https://doi.org/10.3390/curroncol32010029

[21] B. M. Kanber, A. Al Smadi, N. F. Noaman, B. Liu, S. Gou, and M. K. Alsmadi, "Lightgbm: A leading force in breast cancer diagnosis through machine learning and image processing," *IEEE Access*, vol. 12, pp. 39811-39832, 2024. https://doi.org/10.1109/ACCESS.2024.3375755

[22] Y. Yan, P.-H. Conze, M. Lamard, G. Quellec, B. Cochener, and G. Coatrieux, "Towards improved breast mass detection using dual-view mammogram matching," *Medical Image Analysis*, vol. 71, p. 102083, 2021. https://doi.org/10.1016/j.media.2021.102083

[23] M. Ghorbian and S. Ghorbian, "Usefulness of machine learning and deep learning approaches in screening and early detection of breast cancer," *Heliyon*, vol. 9, no. 12, p. e22427, 2023. https://doi.org/10.1016/j.heliyon.2023.e22427

[24] S. Zarif, H. Abdulkader, I. Elaraby, A. Alharbi, W. S. Elkilani, and P. Pławiak, "Using hybrid pre-trained models for breast cancer detection," *Plos One*, vol. 19, no. 1, p. e0296912, 2024. https://doi.org/10.1371/journal.pone.0296912

[25] Q. Fu, W. Xu, X. Zhao, M. Bu, Q. Yuan, and D. Niu, "The microstructure and durability of fly ash-based geopolymer concrete: A review," *Ceramics International*, vol. 47, pp. 29550–29566, 2021.

Edelweiss Applied Science and Technology
ISSN: 2576-8484
Vol. 9, No. 9: 1398-1415, 2025
DOI: 10.55214/2576-8484.v9i9.10138